



Conditional Probabilities for Large Events Estimated by Small Earthquake Rate

YI-HSUAN WU,¹ CHIEN-CHIH CHEN,¹ and HSIEN-CHI LI¹

Abstract—We examined forecasting quiescence and activation models to obtain the conditional probability that a large earthquake will occur in a specific time period on different scales in Taiwan. The basic idea of the quiescence and activation models is to use earthquakes that have magnitudes larger than the completeness magnitude to compute the expected properties of large earthquakes. We calculated the probability time series for the whole Taiwan region and for three subareas of Taiwan—the western, eastern, and northeastern Taiwan regions—using 40 years of data from the Central Weather Bureau catalog. In the probability time series for the eastern and northeastern Taiwan regions, a high probability value is usually yielded in cluster events such as events with foreshocks and events that all occur in a short time period. In addition to the time series, we produced probability maps by calculating the conditional probability for every grid point at the time just before a large earthquake. The probability maps show that high probability values are yielded around the epicenter before a large earthquake. The receiver operating characteristic (ROC) curves of the probability maps demonstrate that the probability maps are not random forecasts, but also suggest that lowering the magnitude of a forecasted large earthquake may not improve the forecast method itself. From both the probability time series and probability maps, it can be observed that the probability obtained from the quiescence model increases before a large earthquake and the probability obtained from the activation model increases as the large earthquakes occur. The results lead us to conclude that the quiescence model has better forecast potential than the activation model.

Key words: Probabilistic forecasting, seismic quiescence, seismic activation, Gutenberg–Richter relation, Taiwan seismicity, ROC test.

1. Introduction

Research on earthquake prediction in the last few decades has increased our understanding of the earthquake process and led to several methods for producing useful estimates of seismic hazards. The

earthquake prediction research here includes three different time intervals: short term from 1 day to a few months, intermediate term from a few months to a few years, and long term from several years to decades. Owing to the limited length of available observations, we have made the most significant progress in intermediate-term prediction research. Many observational studies have shown anomalous seismic behavior such as increases and decreases in the frequency of smaller events (activation/quiescence) preceding a large earthquake (WYSS *et al.* 1990, 1995; WIEMER and WYSS 1994; KOSSOBOKOV *et al.* 1999; HAINZL *et al.* 2000; BEN-ZION and LYAKHOVSKY 2002; OGATA 2004; SAMMIS *et al.* 2004; WU and CHIAO 2006; HUANG 2008; HUANG and DING 2012). These anomalous seismic behaviors can occur a few days to a few years before the occurrence of a large earthquake and continue for several months to a few years (SYKES and JAUMÉ 1990; WIEMER and WYSS 1994; WYSS *et al.* 1995; WU and CHIAO 2006). Precursors, such as activation, quiescence, and foreshocks, shed light on earthquake forecasting; we could determine the potential area that is going to have a large event by detecting and calculating precursory seismicity (TIAMPO *et al.* 2002; CONSOLE *et al.* 2007; WU *et al.* 2008, 2011). However, prediction must include either specific locations, times, and magnitudes or probabilities defined in public terms.

To arrive at a probability estimate for public use, such as public policy and insurance, various approaches have been proposed to calculate the conditional probability (VERE-JONES 1995; FERRAES 2003; GOMBERG *et al.* 2005). For earthquakes, the conditional probability $P(t|\Delta t)$ is the likelihood that a failure will occur in a time period Δt in the future, given that it has not failed before t . The likelihood is based on information regarding past earthquakes in a given area and the basic assumption that future seismic

¹ Department of Earth Sciences, National Central University, No. 300, Jhongda Rd, Jhongli, Taoyuan 32001, Taiwan (R.O.C.). E-mail: yhwu@ncu.edu.tw; maomaowyh@gmail.com

activity will follow that activity pattern observed in the past. The probability distributions of recurrence times, such as the exponential, Weibull, Gamma, and power-law distributions, are typical tools for calculating conditional probabilities (FERRAES 2003). However, various results might be yielded from the above probability distributions; for example, the exponential model might reach the maximum conditional probability for a $m \geq 6.4$ earthquake in the Tokyo area before June 2009, whereas the Weibull model might reach the maximum conditional probability for the same damaging earthquake before October 2129 (FERRAES 2003). In addition, it is difficult to describe all the earthquakes by one probability distribution; for instance, CHEN *et al.* (2012) suggested the use of the Gamma distribution in modeling earthquake interevent times in Taiwan, but WANG *et al.* (2012) showed that the Gamma function is less appropriate to describe the frequency distribution of interevent times for the Taipei metropolitan area in Taiwan compared with the power-law function.

Considering the universality of probability, we use models constructed by RUNDLE *et al.* (2011) that are based on simple models of quiescence and activation for large earthquake probabilities. Quiescence and activation have been discovered in many cases (WYSS *et al.* 1990, 1995; WIEMER and WYSS 1994; KOSSOBOKOV *et al.* 1999; HAINZL *et al.* 2000; BEN-ZION and LYAKHOVSKY 2002; OGATA 2004; SAMMIS *et al.* 2004; WU and CHIAO 2006; HUANG 2008; HUANG and DING 2012) and have also helped us develop some forecast methods (Tiampo *et al.* 2002; HUANG 2004; CHEN and WU 2006; WU *et al.* 2008, 2011; GENTILI 2010). Some research has indicated that activation may be associated with the nucleation of small earthquakes that have a finite probability of growing into a large earthquake, so more small events implies a larger probability for the occurrence of a large earthquake (LANGER 1967; GUNTON and DROZ 1983; GUNTON *et al.* 1983; RUNDLE 1989, 1993; KLEIN and UNGER 1983; RUNDLE *et al.* 1997; SHCHERBAKOV *et al.* 2005). The physics of quiescence may be due to a mechanism such as a critical slowing down (MA 1974; KLEIN and UNGER 1983). When the system is driven to a critical point, fluctuations in systems with long-range interactions, such as elastic systems,

tend to be suppressed prior to large nucleation events. The common point of quiescence and activation is the rate change of earthquakes; therefore, the quiescence and activation models for large earthquakes proposed by RUNDLE *et al.* (2011) are based on the rates of small earthquake activity. They tested these models using earthquake data from the Advanced National Seismic System (ANSS) catalog in California during the years 1985–2011 to determine which model is more consistent with the data. They found that neither the activation nor the quiescence model provides significant forecast skill from the standpoint of a reliability/attributes (R/A) test or a receiver operating characteristic (ROC) test.

We applied quiescence and activation models on earthquake data from the Central Weather Bureau (CWB) in Taiwan. The whole study area is divided into three subareas according to tectonic setting—the western, eastern, and northeastern Taiwan regions. The quiescence and activation models are tested on the whole study area and the three subareas. Furthermore, we divided the subareas into grids and calculated the conditional probability at specific times for every grid point to make two-dimensional maps of the quiescence and activation models so that an area with high probability could be observed. The ROC curves of the probability maps show that the forecast skill of the probability maps is, with few exceptions, beyond the random forecast. The results of both the probability time series and probability maps show that the quiescence model has better forecast skill for large earthquakes and that the high probability yielded by the activation model is more related to aftershocks. Based on our observation, the quiescence model could be a candidate forecast method under the conditions that an adequate interevent time can be obtained and the catalog is consistent.

2. Data

The primary seismicity dataset for Taiwan and nearby islands used in this research is the Central Weather Bureau (CWB) catalog.

The quiescence and activation models involve forecasting large earthquakes of magnitude $m \geq 6$ in

this study using small earthquakes with magnitudes larger than the completeness magnitude. Considering the consistency of the catalog, the quiescence and activation models are examined using the catalog from 1994 to 2013. Nevertheless, a longer catalog from 1973 to 2013 is used for calculating the b value. Because the expected number of small earthquakes, which represents the property of the large earthquakes, is inferred from the b value, the catalog used to calculate the b value has to contain sufficient information; therefore, we adapt the catalog from 1973 to 2013 for calculating the b value. A completeness magnitude $m_c = 3$ can be obtained from both the 1994 to 2013 and the 1973 to 2013 catalogs.

Taiwan is at the complex boundary between the Eurasian Plate and the Philippine Sea Plate (TSAI *et al.* 1977; WU 1978; SHYU *et al.* 2005). Most earthquakes in Taiwan take place in the subduction zone. Because deep earthquakes usually occur offshore and cause less damage than shallow earthquakes in Taiwan, deep earthquakes are not considered in this study. The distribution of earthquake frequency with depth is shown in Fig. 1. The gray solid line shows the cumulative probability of all the earthquakes included in the CWB catalog from 1900 to 2013; the result shows that approximately 90 % of the earthquakes took place above a depth of 30 km.

In addition to the whole Taiwan region, the subareas of Taiwan shown in Fig. 2 are the study

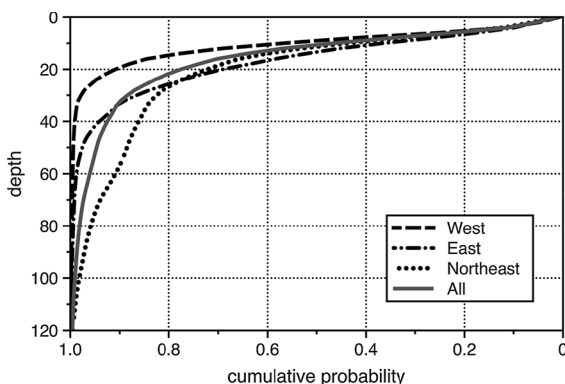


Figure 1

Distribution of earthquake frequency versus depth. The *gray solid line* shows the cumulative probability of all earthquakes from 1900 to 2013. The *black dashed/dash-dotted/dotted line* represents the cumulative probability of earthquakes in the western/eastern/northeastern Taiwan region, as shown in Fig. 2

regions that we are interested in. The subareas are determined according to the seismicity distribution and tectonic setting; they are the western Taiwan region, the eastern Taiwan region, and the northeastern Taiwan region. The distributions of earthquake frequency versus depth for these three study regions are also shown in Fig. 1. The results show that approximately 90 % of the earthquakes occurred above 20 km in the western Taiwan region, approximately 90 % occurred above 30 km in the eastern Taiwan region, and approximately 90 % occurred above 60 km in the northeastern Taiwan region. To sufficiently include the shallow earthquakes and have a uniform cut-off depth for all the study regions, a depth of 40 km is regarded as the cut-off depth.

In Fig. 2, open circles represent the $m \geq 6$ earthquakes that occurred above the cut-off depth from 1900 to 2013. Significantly, there are fewer large earthquakes in the western Taiwan region, and most of them tend to occur in the same place. The major reason these large earthquakes are centered in the same place is that most of the earthquakes are aftershocks, inherently occurring in the same place as

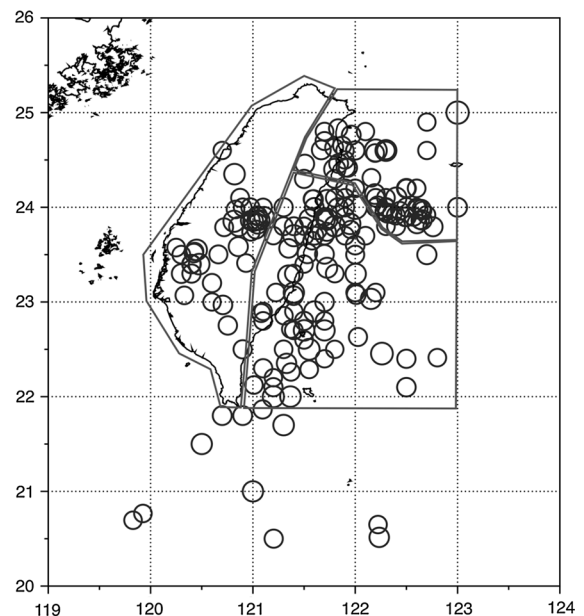


Figure 2

Distribution of $m \geq 6$ earthquakes from 1900 to 2013. *Open circles* represent $m \geq 6$ earthquakes that occurred above the cut-off depth from 1900 to 2013. The *gray lines* show three study regions of interest, which are the western, eastern, and northeastern Taiwan regions

their mainshocks. By including the aftershocks in the calculation of the interevent time, we reduce the real interevent time; however, removing aftershocks may also remove earthquakes that are not aftershocks. Therefore, we calculate the mean interevent time using all the $m \geq 6$ earthquakes that occurred from 1900 to 2013 in order to include more mainshocks.

3. Models

The model of conditional probability of failure for large earthquakes, which is based on the general formalism of reliability or hazard analysis (EBELING 1997; NIST 2010), was developed by RUNDLE *et al.* (2011). The basic idea is to use the small earthquakes that have magnitudes larger than the catalog completeness magnitude m_c to evaluate the conditional probability of a subsequent large earthquake with a magnitude larger than m . The application steps for the time series of the earthquakes are the following:

1. We first calculate the expected number N_C of small earthquakes larger than the catalog completeness magnitude m_c that should be included in a cycle of large earthquakes having magnitudes larger than m by

$$N_C = 10^{b(m-m_c)}. \quad (1)$$

The parameter b is obtained by fitting the seismicity data over a long interval at least 30 years into the past, and b should be a relatively slowly varying function of time over an interval of a year or less.

2. Compute a non-declustered, nonhomogeneous, and time-varying Poisson rate of small earthquakes $v_C(t)$ by a double-averaging method:

$$v_C(t) = \frac{1}{t-t_0} \int_{t_0}^t \frac{\Delta n_C(t)}{T_C} dt. \quad (2)$$

Here, t_0 is the onset of the time period that is going to be examined, T_C is an averaging time, and $\Delta n_C(t)$ is the number of small earthquakes over a time interval $\{t - T_C, t\}$. In RUNDLE *et al.* (2011), T_C is 5 years, which is approximately five times the interevent time of $m \geq 6$ earthquakes in the California region and is obtained by backtesting. Because the main purpose of

our study is to obtain the conditional probability that is spontaneously reflected by the small earthquakes, we use the average interevent time of $m \geq 6$ earthquakes in the corresponding region.

3. Using the average Poisson rate of small earthquakes v_C and the expected number of small earthquakes N_C in a cycle of $m \geq 6$ earthquakes, we can determine a Poisson window:

$$T_W = \frac{N_C}{2v_C}. \quad (3)$$

The Poisson window is a moving time window for sampling the small earthquakes. The ratio of N_C to v_C represents the average time interval between large earthquakes; the sampling frequency $1/T_W$ equals twice the average recurrence frequency, and the factor of 2 in the denominator corresponds to the introduction of the Nyquist frequency.

4. Next, we compute the expected number $n_E(t)$ and observed number $n_O(t)$ of small earthquakes in the Poisson window and their ratio $R(t) = n_O(t)/n_E(t)$. If $R(t) > 1$, there are more small earthquakes observed than were expected during the previous time interval T_W , and the situation corresponds to activation. If $R(t) < 1$, there are fewer small earthquakes observed than were expected during the previous time interval T_W , and the situation corresponds to quiescence. With the definition (1), the expected number of small earthquakes during the time interval T_W is $n_E(t) = N_C/2$. To compute the observed number of small earthquakes $n_O(t)$, a window function of length T_W using tapers on the trailing edge (at time $t - T_W$) is applied over the time series of the small earthquakes. To include the triggering of large events that is sometimes observed during heightened activity at the leading edge time t , a sharp edge is used in the window function:

$$F(t) = \left[\sin \left(\frac{\tau - t + T_W/2}{T_W} \right) \pi + 1 \right], \quad (4)$$

which is valid for $\tau \in \{t - T_W, t\}$. In addition, the window function is normalized so that the area under $F(t)$ is the same as the area under the boxcar window function.

5. With the above equations, two nonhomogeneous Poisson forecast models are constructed: the activation model and the quiescence model. For the activation model, we presume that the conditional probability is higher when the anomalous activity of small earthquakes increases, so the conditional probability is proportional to the ratio $R(t)$ of the observed number of small earthquakes to the expected number of small earthquakes in a Poisson window. The conditional probability of the activation model that a failure will occur in a time Δt in the future, given that it has not failed before t , is given by

$$P_A(t|\Delta t) = 1 - \exp\{-\Delta H_A(t, \Delta t)\}. \quad (5)$$

Here, $\Delta H_A(t, \Delta t)$ is the cumulative conditional hazard rate function of the activation model and equals

$$\Delta H_A(t, \Delta t) = \frac{R(t)fv_C\Delta t}{N_C}. \quad (6)$$

For the quiescence model, we presume that the conditional probability is higher when the anomalous activity of small earthquakes decreases, so the conditional probability is proportional to the inverse of $R(t)$. The conditional probability of the quiescence model that a failure will occur in a time Δt in the future, given that it has not failed before t , is given by

$$P_Q(t|\Delta t) = 1 - \exp\{-\Delta H_Q(t, \Delta t)\}. \quad (7)$$

Here, $\Delta H_Q(t, \Delta t)$ is the cumulative conditional hazard rate function of the quiescence model and equals

$$\Delta H_Q(t, \Delta t) = \frac{fv_C\Delta t}{N_C R(t)}. \quad (8)$$

The parameter f is used to optimize the forecast and make fv_C an optimal Poisson rate. The determination of f relies on standard verification tests (backtesting the forecast).

4. Results and ROC Test

For the quiescence and activation models, the interevent time of large earthquakes is a crucial parameter. We calculated the interevent times of $m \geq 6$ earthquakes that occurred from 1900 to 2013 within depths of 0 to 40 km and obtained an average interevent time of approximately 0.55 years.

Considering the complexity of the tectonics and the different loading rate in Taiwan, we divided the study region into three subareas, which are western Taiwan, northeastern Taiwan, and eastern Taiwan (Fig. 2), and we grouped the earthquakes according to their locations. The average interevent times of $m \geq 6$ earthquakes at shallow depths of 0–40 km for the western, northeastern, and eastern Taiwan regions are approximately 2.65, 2.04, and 1.25 years, respectively. The b values obtained by fitting the Gutenberg–Richter scaling law to earthquakes with magnitudes larger than the cut-off magnitude m_c for the whole, western, northeastern, and eastern Taiwan regions are approximately 1.07, 0.95, 1.03, and 1.02, respectively.

We took 0.01 years as a time step to compute the conditional probabilities for four different study regions; Fig. 3a–d, respectively, show the results for the whole, western, eastern, and northeastern Taiwan regions. The conditional probabilities P_Q and P_A for $m \geq 6$ earthquakes that will occur within 30 days yielded from the quiescence and activation models are shown in the middle and upper panels of Fig. 3, and $m \geq 5$ earthquake sequences are shown in the bottom panels. The vertical dashed lines indicate the times of the $m \geq 6$ earthquakes. The gray lines indicate the mean probabilities obtained from the quiescence and activation models for each study region from 1994 to 2013, and the gray-colored bands show the range from the mean value to a standard deviation. The parameter f in the previous work of RUNDLE *et al.* (2011) is determined by optimizing the forecast using standard verification tests; thus, fv_C is considered to be an optimal Poisson rate. Instead of considering an optimal Poisson rate, we took a uniform f and considered v_C to be an inherently generated rate.

Comparing P_Q and P_A in Fig. 3, the probability time series obtained from the activation model shows a contrary result to the quiescence model when it approaches a large ($m \geq 6$) event and just after a large event occurs. It can be easily observed that P_A typically trends lower than the mean value when an $m \geq 6$ earthquake approaches, sharply increases as the event occurs, and reaches its highest value just after the earthquake occurs. In some cases, the increase of P_A from the mean value can be several

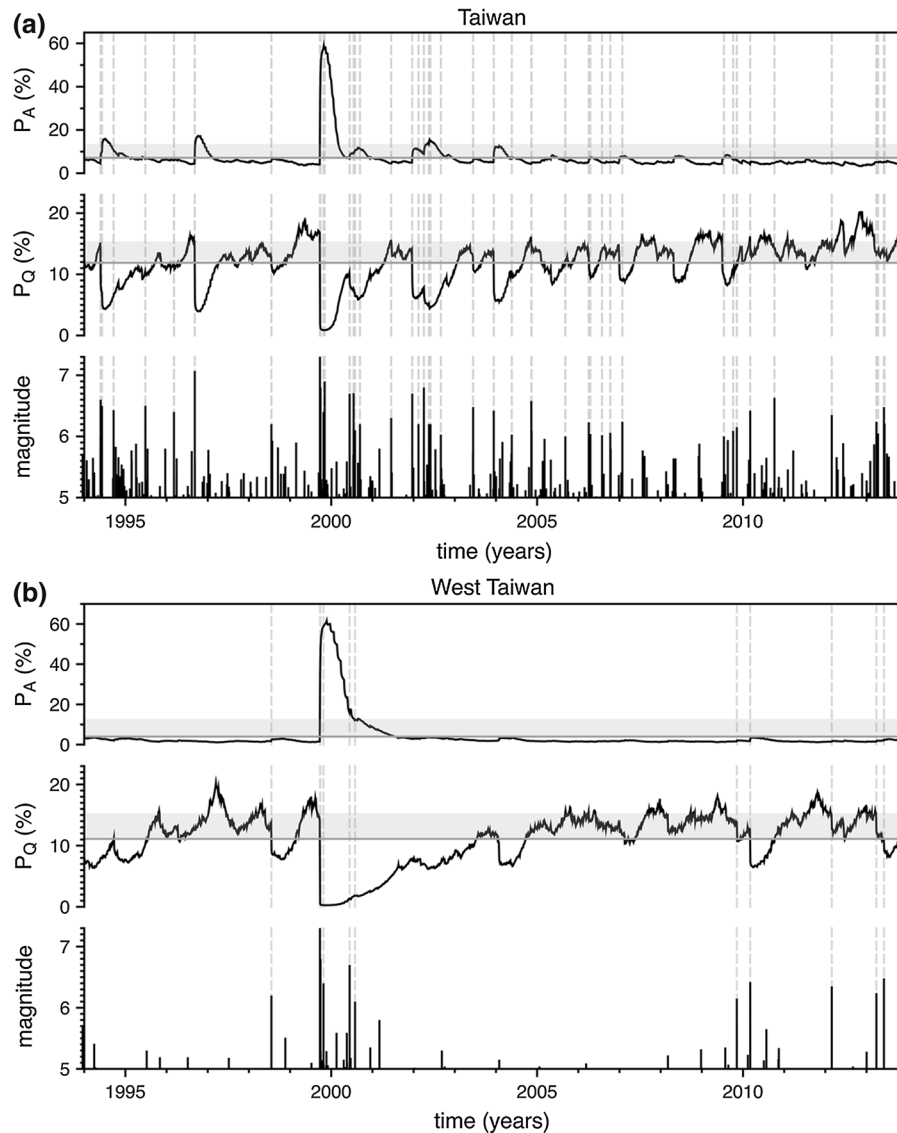


Figure 3

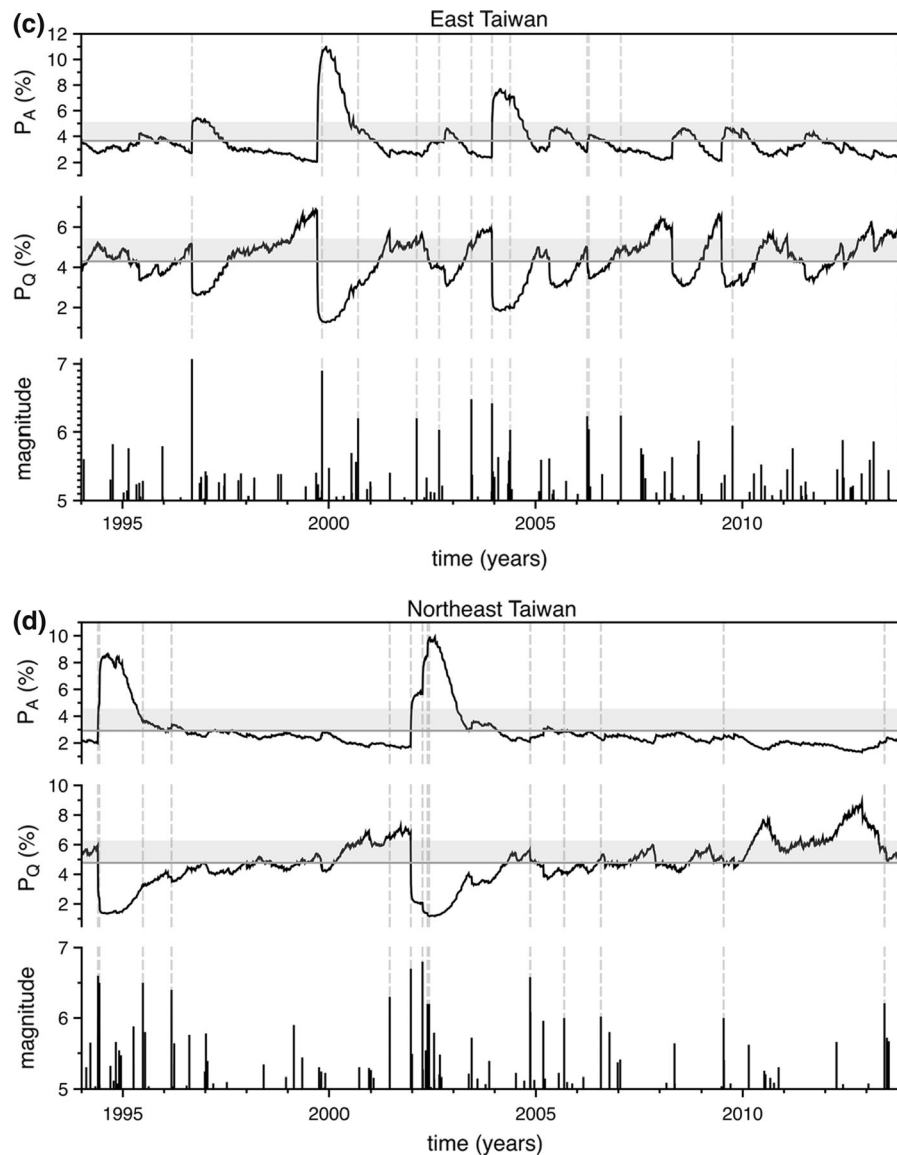
Time series of 30-day forecasts for **a** the whole Taiwan region, **b** the western Taiwan region, **c** the eastern Taiwan region, and **d** the northeastern Taiwan region from 1994 to 2013. The *top panel* of each figure shows the 30-day conditional probability obtained from the activation model as a function of time. The *middle panel* of each figure shows the 30-day conditional probability obtained from the quiescence model as a function of time. The *bottom panel* of each figure shows $m \geq 5$ earthquake sequences. The *dashed vertical lines* indicate the times of $m \geq 6$ earthquakes

times the standard deviation. By contrast, P_Q typically increases when an $m \geq 6$ earthquake approaches, sharply decreases as the earthquake occurs, and reaches its lowest value after the earthquake occurs. Most exceptions to this pattern occur when the $m \geq 6$ earthquakes are clustered in time.

In the whole, western, and eastern Taiwan regions (Fig. 3a–c), most $m \geq 6$ earthquakes occur after P_Q

increases beyond one standard deviation (3.5, 4.2, and 1.1). However, in the northeastern Taiwan region, the increase of P_Q is usually less than one standard deviation (1.5) except for the clustered events in 1994, 2002, and 2013.

An extremely high P_A value, 60 %, which is about 8 times the mean value, was yielded after the 1999 Chi–Chi ($m = 7.3$) earthquake, as can be

Figure 3
continued

observed in Fig. 3a. This extreme value can also be observed in Fig. 3b, c because of the Chi-Chi mainshock and its aftershocks in the western Taiwan region and some aftershocks in the eastern Taiwan region. Due to the effect of the Chi-Chi mainshock, the pattern that P_Q increases just before a large earthquake is not shown for the large earthquakes that are clustered with the Chi-Chi mainshock; in addition, an increase of P_Q before the cluster of events in 2000 is not clear as for other events.

The activation and quiescence models also produce some false alarms where P_Q increases and then sharply decreases while P_A decreases and then sharply increases but there is no corresponding $m \geq 6$ earthquake. Some cases, such as the one that occurs in mid 2008 in the whole Taiwan region (Fig. 3a), the one that occurs in early 2004 in the western Taiwan region (Fig. 3b), and the ones that occur in early 2005 and mid 2008 in the eastern Taiwan region (Fig. 3c), are even preceded by an

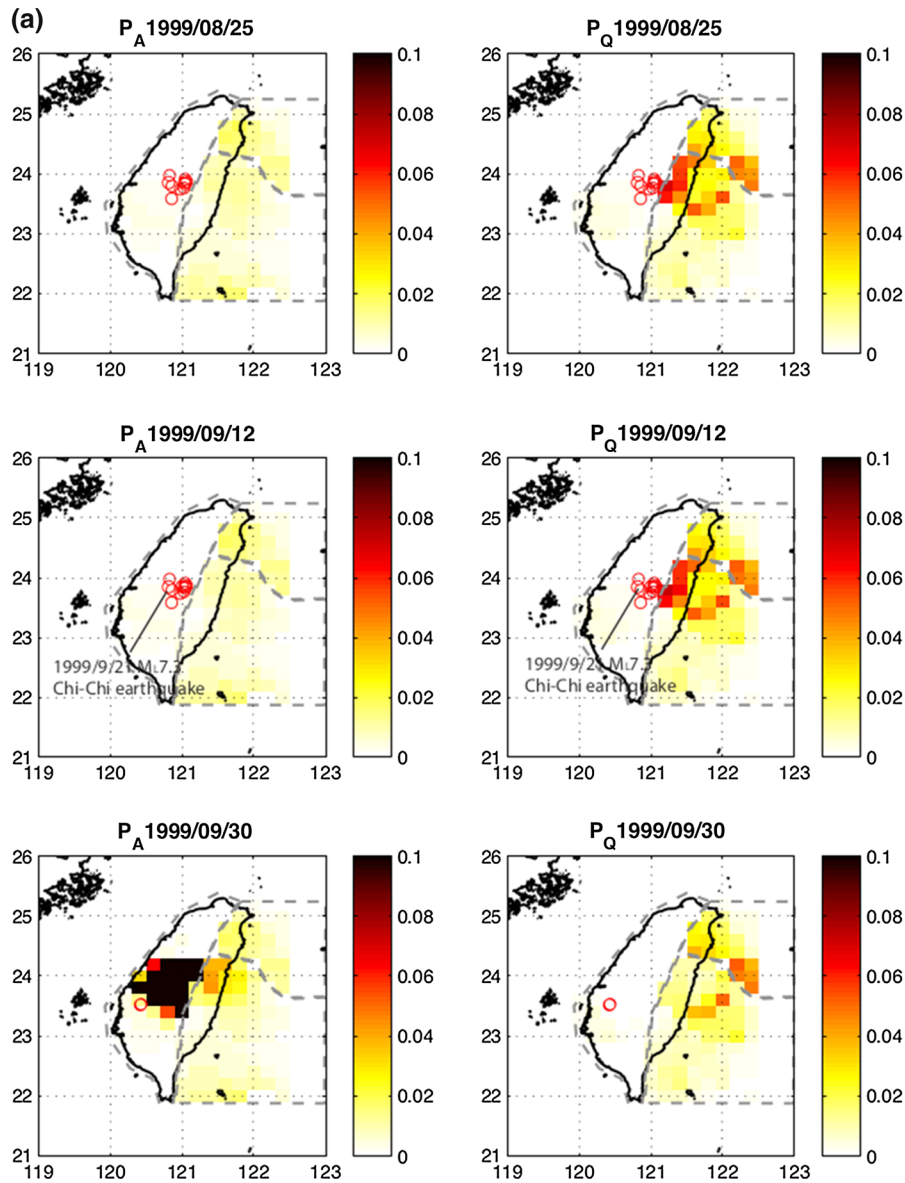


Figure 4

Maps of conditional probability for the quiescence and activation models at specific times that are close to **a** the 1999 Chi–Chi earthquake, **b** the 2003 Chengkung earthquake, and **c** the 2010 Jiashian earthquake. The *left panels* of each figure represent the conditional probabilities obtained from the activation model, and the *right panels* of each figure represent the conditional probabilities from the quiescence model for the grids in the study region at the labeled time. The *top/middle/bottom panels* of each figure show the conditional probability taken before/just before/after the large event. The *red circles* are the $m \geq 6$ earthquakes that occur within 30 days of the time labeled at the *top* of each panel.

The Chi–Chi, Chengkung, and Jiashian earthquakes are indicated in the *middle panel* of each figure

increase of P_Q that is beyond one standard derivation.

The probability in Fig. 3 is a coherent property of every single region rather than of an individual location. To look into the probability change of individual locations in the study regions, we

applied the probability calculation to every grid point in the study regions. We divided the research area of $119.5\text{--}122.5^\circ\text{E}$ and $21.5\text{--}25.5^\circ\text{N}$ into 300 nonoverlapping $0.2^\circ \times 0.2^\circ$ square boxes and took the centers of the boxes in the study region as the grid points. For every grid point, the conditional

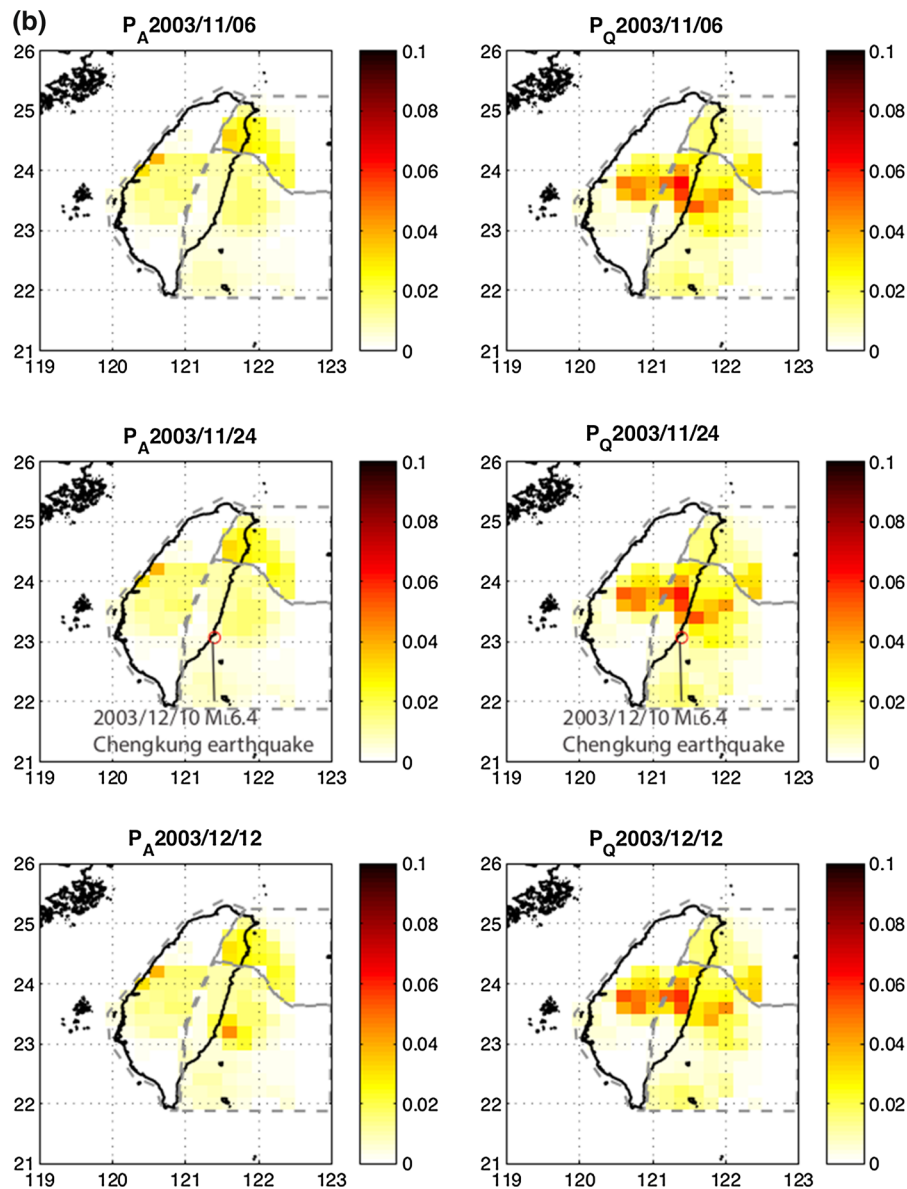


Figure 4
continued

probability was calculated using the events within a distance of 50 km from the grid point and in the subregion where the grid point lies. Considering $m \geq 6$ earthquakes to be large earthquakes, earthquakes with magnitudes larger than the catalog completeness magnitude $m_c = 3$ to be small earthquakes, and the time step to be 0.01 years, the probability time series obtained from the quiescence and activation models for every grid point

are shown in Fig. 4. Given a specific time, the probabilities for the quiescence and activation models that an $m \geq 6$ earthquake occurs within 30 days after the specific time were then mapped as shown in Fig. 4.

Figure 4a–c show the probability maps before and after the 1999 Chi–Chi ($m = 7.3$) earthquake, the 2003 Chengkung ($m = 6.6$) earthquake, and the 2010 Jiashian ($m = 6.4$) earthquake. The middle panels of

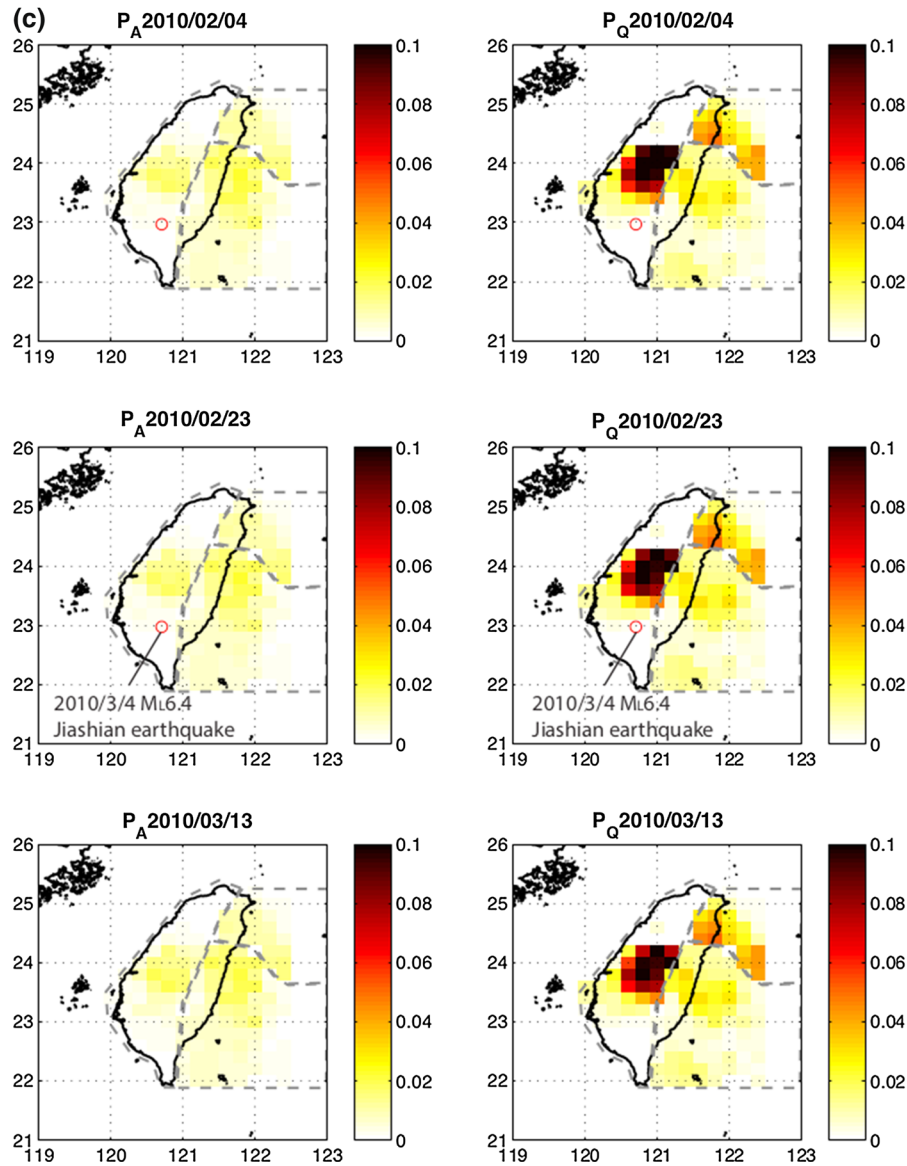


Figure 4
continued

Fig. 4a–c represent the probability maps just before the earthquakes. The locations of $m \geq 6$ earthquakes that occur within 30 days after the time labeled at the top of the figures are shown as red open circles. The probability of the quiescence and activation models is denoted by P_Q and P_A and is colored in the map; the warmer the color, the higher the probability.

In Fig. 4a, some high P_A and P_Q were yielded around the epicenter of the Chi–Chi earthquake

before the event occurred; however, high P_A and P_Q were only yielded in the eastern Taiwan region, not in the western Taiwan region. After the Chi–Chi earthquake, the P_A around the epicenter became very high in the western Taiwan region, and the P_Q near the epicenter in the eastern Taiwan region decreased a lot. In Fig. 4b, high P_Q can be observed north of the Chengkung earthquake before the event occurred, and the P_Q decreased after the event. By contrast,

high P_A around the epicenter was absent before the event and showed up after the event. Compared with Fig. 4a, b, Fig. 4c does not show changes in P_Q before and after the Jiashian earthquake; in addition, the distribution of high P_Q in the western Taiwan region is consistent with the distribution of the Chi-Chi earthquake and its aftershocks.

Considering that the probability maps (Fig. 4) may vary with the threshold we give in the color bar, we apply the receiver operating characteristics (ROC) test to estimate the reliability of the probability maps. A ROC curve is a graphical plot that illustrates the performance of a binary classifier system, as its discrimination threshold is varied in signal detection theory (GREEN and SWETS 1966). A ROC curve is generally employed in medical science and social science; it is also a useful tool for evaluation of machine learning techniques (ZWEIG and CAMPBELL 1993; PEPE 2003; OBUCHOWSKI 2003). The task of the ROC curve in these fields is mostly to increase the prediction of a model or to evaluate the accuracy of the default probability model.

The ROC curve has been increasingly used in verifying probability forecasts because of the binary characteristics yielded from the probability forecast, i.e., the hit rate (HR) and false alarm rate (FR). In the ROC test, a threshold R is applied to the 2D map of conditional probability to transform the forecast into a binary forecast. For a given threshold R , boxes with probability $P(i|\Delta t) \geq R$ represent the forecast locations, and boxes with large future earthquakes that occur during the forecast period represent the event locations. A forecast is successful when it makes a forecast location on an event location, and the forecast is a false alarm when it makes a forecast location on a box that is not an event location. The fraction of successful forecasts out of the total event locations is the hit rate (HR), and the fraction of false alarms out of the total boxes that are not event locations is the false alarm rate (FR). The ROC diagram is then constructed by plotting HR against FR as the threshold value R decreases.

To evaluate the performance of the activation and quiescence models in time and space at the same time, we calculated an average ROC curve over a set of conditional probability maps (Fig. 5). We sampled the time period from 2001 to 2010 by 0.05 years, and

calculated a conditional probability map for the activation model at each sampled time as well as for the quiescence model, then finally averaged all the ROC curves. The black lines in Fig. 5 show the results for taking $m \geq 6$ earthquakes as target earthquakes, and the gray lines show the results for $m \geq 5$ earthquakes. The dotted lines are ROC curves of 100 bootstrap tests for taking $m \geq 6$ earthquakes as target earthquakes, and the dashed lines are the results of bootstrap tests for $m \geq 5$ earthquakes.

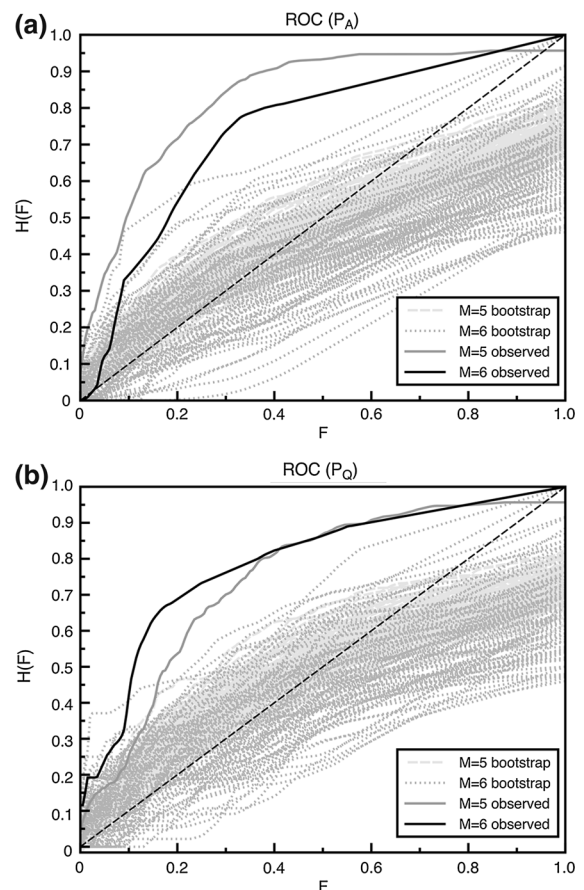


Figure 5

Receiver operating characteristic diagrams of the conditional probability map for **a** the activation model and **b** the quiescence model. The *black solid line* and *gray solid line* denote the averaged ROC curves of the conditional probability map for $m \geq 6$ and $m \geq 5$ earthquakes that occur in 30 days after the sampled times during 2001 to 2010. The *dotted* and *dashed lines* are ROC curves of the 100 bootstrap tests for the $m \geq 6$ and $m \geq 5$ earthquakes. The *diagonal line* from the *lower-left corner* (no hits or false alarms) to the *upper-left corner* (no false alarms, only successful forecasts) represents no skill (random forecast). The closer an ROC curve is to the *upper-left corner*, the higher the forecast skill

The upper-left corner of the ROC diagram represents a perfect forecast system (no false alarms, only successful forecasts). The lower-left corner (no hits or false alarms) represents a system that never warns of an event. The upper-right corner represents a system where the event is always warned. A random forecast is characterized by the condition $HR = FR$, which is represented on the ROC diagram by a diagonal line connecting the point at the lower-left corner to the point at the upper-right corner. A good forecast should always make more successful forecasts than false alarms; therefore, the closer any ROC curve is to the upper-left corner, the higher its forecast skill.

5. Discussion and Conclusions

One main purpose of this study is to look for an alternative forecast method for large earthquakes. The quiescence and activation models proposed by RUNDLE *et al.* (2011) were examined on the CWB catalog. In addition to the probability time series for the entire Taiwan region and the three subregions, we also made probability maps. From both the probability time series and the probability maps, it is significant that the quiescence model has better forecasting skill because of the increasing probability before the large events in the time series and the high probability distributed around the epicenter. In contrast to the quiescence model, the activation model does not have increasing probability before the event or high probability distributed around the event, but it does after the event. Because high P_A is distributed around the epicenter, the high probability of the activation model after the event should be associated with aftershocks.

The probability map enables the quiescence and activation models to identify locations with high probability; furthermore, the probability maps demonstrate that the sharply increasing P_Q or P_A in the time series is dominated by the seismicity around the epicenter of the large event before and after the event. Take the Chengkung earthquake as an example (Fig. 4b); except for the P_Q north of the epicenter, all the other P_Q remain the same before and after the event.

The properties of the seismicity associated with the large event can be observed not only in the probability maps but also in the probability time series. The probability P_Q usually drops as soon as $m \geq 6$ events occur in the eastern Taiwan region (Fig. 3c), except for two events that occurred in late 1999 and late 2009. For these two special events, some $6 > m > 5$ earthquakes occurred just before the $m \geq 6$ events, and the probability P_Q drops as the $m > 5$ earthquakes occur. Because the last $m \geq 6$ event of these two special events occurred at least 2 years earlier, the results suggest a high possibility that the $6 > m > 5$ earthquakes preceding these two special events are the foreshocks of these two special events. Another interesting characteristic reflected in the P_A and P_Q is the clustering of events in the northeastern Taiwan region. In Fig. 3d, it can be observed that P_Q only increased significantly prior to two clusters that occurred in mid 1994 and mid 2002, and P_A increased progressively to the highest value in these two clusters. Unlike most $m \geq 6$ earthquakes that took place offshore in the northeastern Taiwan region, the first two $m \geq 6$ earthquakes in 1994 took place very close to each other in time and space, and then the third $m \geq 6$ earthquake occurred at Yilan within one month. The cluster that caused high P_A and P_Q in 2002 included four $m \geq 6$ earthquakes, three of which were offshore earthquakes and the fourth at Yilan.

The ROC curves of P_A and P_Q (Fig. 5) show the significance of the activation and quiescence models. It can be observed that the probability maps of the quiescence model have better forecast ability than the activation model when taking $m \geq 6$ earthquakes as the target earthquakes. However, the probability maps of the quiescence model do not offer a better forecast than the activation model when taking $m \geq 5$ earthquakes as the target earthquakes. Because P_A usually decreases before the large events while P_Q increases and then sharply increases when the event occurs while P_Q decreases, P_A would have high value just before the $m \geq 5$ earthquakes following another large event and P_Q would have low value in this case. As a consequence, the quiescence model shows better forecasting skill as a forward forecast tool.

It is worth noting that the ROC curve in this study is not just a ROC curve of conditional probability at a

single time but an averaged ROC curve of the conditional probability map over a time span. RUNDLE *et al.* (2011) carried out the ROC test on the time series of activation and quiescence models using the whole catalog in California and Nevada; in this study, we carried out the ROC test on the probability map on which only earthquakes with a distance smaller than 50 km from the grid point were considered. The ROC curves in California show a diagonal trend (Fig. 4 in RUNDLE *et al.* 2011); however, the average ROC curves in Taiwan show a trend that is close to the upper-left corner of the ROC diagram. The activation and quiescence models do not show significance in the ROC test in RUNDLE *et al.* (2011) because the models usually fail to forecast the events that are clustered closely in time even when these events are distant from each other in space. The events that are clustered in time but distant in space may be taken as distinct events in the probability map, therefore the significance of the activation and quiescence models can be observed in our average ROC curve.

Acknowledgments

The authors would like to express their gratitude to the Central Weather Bureau (CWB) for providing their quality earthquake catalogs and to Chien-Hsin Chang for providing the information about the catalog. The work of Y.-H.W. and C.-C.C. was supported by the National Science Council (ROC) (grant NSC-102-2811-M-008-075) and the Department of Earth Sciences, NCU (ROC).

REFERENCES

- BEN-ZION, Y., and LYAKHOVSKY, V. (2002), *Accelerated Seismic Release and Related Aspects of Seismicity Patterns on Earthquake Faults*, Pure Appl. Geophys. 159, 2385–2412.
- CHEN, C.C., and WU, Y.H. (2006), *An Improved Region-Time-Length Algorithm Applied to the 1999 Chi-Chi, Taiwan Earthquake*, Geophys. J. Int. 166, 1144–1147.
- CHEN, C.H., WANG, J.P., WU, Y.M., CHAN, C.H., and, CHANG, C.H. (2012), *A Study of Earthquake Inter-Occurrence Times Distribution Models in Taiwan*, Nat. Hazards. 69, 1335–1350.
- CONSOLE, R., MURRU, M., CATALLI, F., and FALCONE, G. (2007), *Real Time Forecasts through an Earthquake Clustering Model Constrained by the Rate-and-State Constitutive Law: Comparison with a Purely Stochastic ETAS Model*, Seismol. Res. Lett. 78, 49–56.
- EBELING, C.E., *An Introduction to Reliability and Maintainability Engineering*, (McGraw-Hill, Boston 1997).
- FERRAES, S.G. (2003), *The Conditional Probability of Earthquake Occurrence and the Next Large Earthquake in Tokyo, Japan*, J. Seismol. 7, 145–153.
- GENTILI, S. (2010), *Distribution of Seismicity before the Larger Earthquakes in Italy in the Time Interval 1994–2004*, Pure Appl. Geophys. 167, 933–958.
- GREEN, D.M., and SWETS, J.A., *Signal Detection Theory and Psychophysics* (Wiley, New York 1966).
- GOMBERG, J., BELARDINELLI, M.E., COCCO, M., and REASENBERG, P. (2005), *Time-Dependent Earthquake Probabilities*, J. Geophys. Res. 110, B05S04, doi:10.1029/2004JB003405.
- GUNTUN, J.D., and DROZ, M., *Introduction to the Theory of Metastable and Unstable States* (Springer-Verlag, Berlin 1983).
- GUNTUN, J.D., SAN MIGUEL, M., and SAHNI, P.S., The dynamics of first order phase transitions, *Phase Transitions and Critical Phenomena*, (eds. Domb, C., and Lebowitz, J.) (Academic, London 1983) pp. 269–467.
- HAINZL, S., ZÖLLER, G., KURTHS, J., and ZSCHAU, J. (2000), *Seismic Quiescence as an Indicator for Large Earthquakes in a System of Self-Organized Criticality*, Geophys. Res. Lett. 27, 597–600.
- HUANG, Q.H. (2004), *Seismicity Pattern Changes Prior to Large Earthquakes-An Approach of the RTL Algorithm*, Terr. Atmos. Ocean. Sci. 15, 469–491.
- HUANG, Q.H. (2008), *Seismicity Changes prior to the M_S 8.0 Wenchuan Earthquake in Sichuan, China*, Geophys. Res. Lett. 35, L23308, doi:10.1029/2008GL036270.
- HUANG, Q.H., and DING, X. (2012), *Spatiotemporal Variations of Seismic Quiescence prior to the 2011 M 9.0 Tohoku Earthquake Revealed by an Improved Region-Time-Length Algorithm*, Bull. Seismol. Soc. Am. 102, 1878–1883.
- KLEIN, W., and UNGER, C. (1983), *Pseudospinodals, Spinodals and Nucleation*, Phys. Rev. B 28, 445–448.
- KOSSOBOKOV, V.G., MAEDA, K., and UYEDA, S. (1999), *Precursory Activation of Seismicity in Advance of the Kobe, 1995, $M=7.2$ Earthquake*, Pure Appl. Geophys. 155, 409–423.
- LANGER, J.S. (1967), *Theory of the Condensation Point*, Ann. Phys. 41, 108–157.
- MA, S.K., *Modern Theory of Critical Phenomena* (Benjamin-Cummings, Reading, MA 1974).
- NIST/SEMATECH e-Handbook of Statistical Methods, 2010. Available at: <http://www.itl.nist.gov/div898/handbook/> (last accessed June 2012).
- OBUCHOWSKI, N.A. (2003), *Receiver Operating Characteristic Curves and Their Use in Radiology*, Radiology 229, 3–8.
- OGATA, Y. (2004), *Seismicity Quiescence and Activation in Western Japan Associated with the 1944 and 1946 Great Earthquakes near the Nankai Trough*, J. Geophys. Res. 109, B04305, doi:10.1029/2003JB002634.
- PEPE, M.S., *The Statistical Evaluation of Medical Tests for Classification and Prediction* (Oxford, New York 2003).
- RUNDLE, J.B. (1989), *A Physical Model for Earthquakes. 3. Thermodynamical Approach and Its Relation to Nonclassical Theories of Nucleation*, J. Geophys. Res. 94, 2839–2855.
- RUNDLE, J.B. (1993), *Magnitude-Frequency Relations for Earthquakes Using a Statistical-Mechanical Approach*, J. Geophys. Res. 98, 21 943–21 949.
- RUNDLE, J.B., GROSS, S., KLEIN, W., and TURCOTTE, D.L. (1997), *The Statistical Mechanics of Earthquakes*, Tectonophysics 277, 147–164.

- RUNDLE, J.B., HOLLIDAY, J.R., YODER, M., SACHS, M.K., DONNELLAN, A., TURCOTTE, D.L., TIAMPO, K.F., KLEIN, W., and KELLOGG, L.H. (2011), *Earthquake Precursors: Activation or Quiescence?* Geophys. J. Int. 187, 225–236.
- SAMMIS, C.G., BOWMAN, D.D., and KING, G. (2004), *Anomalous Seismicity and Accelerating Moment Release Preceding the 2001 and 2002 Earthquakes in Northern Baja California, Mexico*, Pure Appl. Geophys. 161, 2369–2378.
- SHICHERBAKOV, R., YAKOVLEV, G., TURCOTTE, D.L., and RUNDLE, J.B. (2005), *Model for the Distribution of Aftershock Interoccurrence Times*, Phys. Rev. Lett. 95, 218501, doi:[10.1103/PhysRevLett.95.218501](https://doi.org/10.1103/PhysRevLett.95.218501).
- SHYU, J.B.H., SIEH, K., CHEN, Y.G., and LIU, C.S. (2005), *Neotectonic Architecture of Taiwan and Its Implications for Future Large Earthquakes*, J. Geophys. Res. 110, B08402, doi:[10.1029/2004JB003251](https://doi.org/10.1029/2004JB003251).
- SYKES, L.R., and JAUMÉ, S.C. (1990), *Seismic Activity on Neighbouring Faults as a Long-Term Precursor to Large Earthquakes in the San Francisco Bay Area*, Nature 348, 595–599.
- TIAMPO, K.F., RUNDLE, J.B., MCGINNIS, S.A., and KLEIN, W. (2002), *Pattern Dynamics and Forecast Methods in Seismically Active Regions*, Pure Appl. Geophys. 159, 2429–2467.
- TSAI, Y.B., TENG, T.L., CHIU, J.M., and LIU, H.L. (1977), *Tectonic Implications of the Seismicity in the Taiwan Region*, Mem. Geol. Soc. China 2, 13–41.
- VERE-JONES, D. (1995), *Forecasting Earthquakes and Earthquake Risk*, Int. J. Forecasting 11, 503–538.
- WANG, J.H., CHEN, K.C., LEE, S.J., HUANG, W.G., WU, Y.H., and LEU, P.L. (2012), *The Frequency Distribution of Inter-Event Times of $M \geq 3$ Earthquakes in the Taipei Metropolitan Area: 1973–2010*, Terr. Atmos. Ocean. Sci. 23, 269–281.
- WIEMER, S., and WYSS, M. (1994), *Seismic Quiescence before the Landers ($M = 7.5$) and Big Bear ($M = 6.5$) 1992 Earthquakes*, Bull. Seismol. Soc. Am. 84, 900–916.
- WU, F.T. (1978), *Recent Tectonics of Taiwan*, J. Phys. Earth 2, S265–S299.
- WU, Y.H., CHEN, C.C., and RUNDLE, J.B. (2008), *Precursory Seismic Activation of the Pingtung (Taiwan) Offshore Doublet Earthquakes on 26 December 2006: a Pattern Informatics Analysis*, Terr. Atmos. Ocean. Sci., 19, 743–749.
- WU, Y.H., CHEN, C.C., and RUNDLE, J.B. (2011), *Precursory Small Earthquake Migration Patterns*, Terra Nova, 23, 369–374.
- WU, Y.M., and CHIAO, L.Y. (2006), *Seismic Quiescence before the 1999 Chi-Chi, Taiwan, M_W 7.6 Earthquake*, Bull. Seismol. Soc. Am. 96, 321–327.
- WYSS, M., BODIN, P., and HABERMANN, R.E. (1990), *Seismic Quiescence at Parkfield: an Independent Indication of an Imminent Earthquake*, Nature 345, 426–428.
- WYSS, M., WESTERHAUS, M., BERCKHEMER, H., and ATEs, R. (1995), *Precursory Seismic Quiescence in the Mudurnu Valley, North Anatolian Fault Zone, Turkey*, Geophys. J. Int. 123, 117–124.
- ZWEIG, M.H., and CAMPBELL, G. (1993), *Receiver-Operating Characteristic (ROC) Plots: a Fundamental Evaluation Tool in Clinical Medicine*, Clin. Chem. 39, 561–577.

(Received August 12, 2014, revised November 26, 2014, accepted December 15, 2014, Published online January 23, 2015)